

DOI: 10.1002/cplu.201300306

Solid-State Properties and Vibrational Circular Dichroism Spectroscopy in Solution of Hybrid Foldamers Stereoisomeric Mixtures

Nicola Castellucci,^[a] Giuseppe Falini,^[a] Lorenzo Milli,^[a] Magda Monari,^[a] Sergio Abbate,^[b, c] Giovanna Longhi,^[b, c] Ettore Castiglioni,^[b, d] Giuseppe Mazzeo,^[b] and Claudia Tomasini^{*[a]}

Upon slow evaporation of a 1:1 diastereoisomeric mixture of Boc-(L-Phe-L-Oxd)₂-OBn (**1**; Boc = *tert*-butyloxycarbonyl; L-Oxd = *trans*-(4*S*,5*R*)-4-carboxy 5-methyloxazolidin-2-one, Bn = benzyloxycarbonyl) and Boc-L-Phe-L-Oxd-D-Phe-L-Oxd-OBn (**2**) in methyl *tert*-butyl ether, single crystals suitable for an X-ray diffraction study were obtained. In contrast, the two pure oligomers lead to the formation of amorphous solids under any crystallization conditions. The preferential conformation of both oligomers was fully elucidated in the solid phase and compared with the known conformation of Boc-(L-Phe-D-Oxd)₂-OBn (**3**). The preferred conformation of **1** ranges from a polyproline II (PPII) helix to β strands and we can gather that

longer and more structured oligomers will form PPII helices. In contrast, compound **3** forms infinite antiparallel β -sheet structures; thus showing the strong effect of the reversal of the absolute configuration of the Oxd moieties on the secondary structure of these hybrid foldamers. The same outcome was retained in solution, as demonstrated by vibrational circular dichroism analysis. Finally, we have demonstrated that a 1:1 mixture of **1** and **2** leads to the formation of new materials with interesting properties that are missing from the two pure compounds, such as the tendency to form crystals, fibers, and globules, depending on the solvent.

Introduction

Foldamers are unnatural oligomers able to adopt a preferred secondary structure and have become the focus of a very active area of chemical research. The essential requirement of a foldamer is to possess a well-defined, repetitive secondary structure, which is dictated by conformational preferences of the monomeric units, attractive and/or repulsive noncovalent intramolecular interactions, and solvent effects.^[1] Before the term “foldamer” was coined, many nucleic acid analogues and peptide analogues had already been successfully designed to mimic the structures and, potentially, the biological properties of their natural counterparts.

In 2001, Moore et al. divided foldamers into two large families:^[2] “biotic” foldamers, the backbones of which are chemically related to biopolymers (nucleotidomimetic and peptidomimetic foldamers); and “abiotic” foldamers, which emanate from a bottom-up approach (for example, aromatic foldamers); this classification was exploited and emphasized by Guichard and Huc in a recent review.^[3]

Recently, we described the synthesis and conformational analysis of the foldamers Boc-(L-Phe-L-Oxd)_{*n*}-OBn (*n* = 1–6; Boc = *tert*-butyloxycarbonyl; L-Oxd = *trans*-(4*S*,5*R*)-4-carboxy 5-methyloxazolidin-2-one; Bn = benzyloxycarbonyl).^[4] The synthesis was performed by conventional methods in solution and conformational analysis was performed by means of IR, ¹H NMR, electronic circular dichroism (ECD), and vibrational circular dichroism (VCD) spectroscopy; ab initio calculations in the case of *n* = 1 provided a physical insight into the conformational properties.

Employing VCD spectroscopy, we could demonstrate that the structural behavior of the oligomers Boc-(L-Phe-L-Oxd)_{*n*}-OBn was similar from *n* = 2 to *n* = 6; ECD spectra suggest the presence of different conformations between *n* = 1, on one side, and longer chain foldamers, on the other side, owing to the significant shift towards shorter wavelengths with increasing chain length. VCD and absorption IR spectra in CCl₄ could be interpreted as indicative of a polyproline II (PPII) structure in the case of short Boc-L-Phe-L-Oxd-OBn because detailed DFT computational analysis allowed us to demonstrate that the most populated conformers exhibited backbone dihedral angles similar to those of a PPII geometry. The conformational

[a] Dr. N. Castellucci, Prof. G. Falini, Dr. L. Milli, Prof. M. Monari, Prof. C. Tomasini
Dipartimento di Chimica “G. Ciamician”
Alma Mater Studiorum, Università di Bologna
Via Selmi 2, 40126 Bologna (Italy)
E-mail: claudia.tomasini@unibo.it

[b] Prof. S. Abbate, Prof. G. Longhi, Dr. E. Castiglioni, Dr. G. Mazzeo
Dipartimento di Medicina Molecolare e Traslazionale
Università degli Studi di Brescia
Viale Europa 11, 25123 Brescia (Italy)

[c] Prof. S. Abbate, Prof. G. Longhi
CNISM, Consorzio Interuniversitario Scienze Fisiche della Materia
Via della Vasca Navale 84, 00146 Roma (Italy)

[d] Dr. E. Castiglioni
JASCO Europe, Via Cadorna 1
23894 Cremella (LC) (Italy)

 Supporting information for this article is available on the WWW under <http://dx.doi.org/10.1002/cplu.201300306>.

assignment of longer oligomers, which were dissolved in methanol, was more complicated because, in these cases, mixtures of conformers were present in solution; nevertheless, a PPII conformation could be taken into account. This outcome is very different from the results obtained with other oligomers, in which the D-Oxd moiety is alternated with L-amino acids: Boc-(L-Ala-D-Oxd)_n-OBn^[5] and Boc-[(S)-β³-hPhg-D-Oxd]_n-OR ((S)-β³-hPhg = (S)-β³-homophenylglycine)^[6] oligomers form H₁₀ or H₁₁ helices, respectively.

As in the case of the Boc-(L-Phe-L-Oxd)_n-OBn series, we were not able to grow crystals suitable for single-crystal X-ray diffraction, so we tried to grow suitable crystals from a solution of diastereoisomers.

It is known that the crystallization of enantiomerically pure chiral molecules is more difficult than the crystallization of the corresponding racemate.^[7] Recently, racemic crystallization and X-ray crystallography has been successfully applied to the determination of the unknown structure of snow flea antifreeze protein (sfAFP).^[8] It is still not clear whether more facile crystallization of racemic protein mixtures is a general phenomenon, as predicted by Wukovitz and Yeates,^[9] but this phenomenon has been extensively studied for proteins, short peptides^[10] and, more recently, foldamers.^[11]

Balaram and co-workers determined the crystal structures of seven tripeptides in enantiomeric and racemic forms.^[12] They demonstrated that the two enantiomeric peptides and racemates might have crystallized in two different polymorphic forms, although the preferred conformations of the tripeptides were very similar.

In contrast, the variation of properties in the solid state (including the tendency to crystallize) for a mixture of diastereoisomers, compared with pure compounds, has been less described.^[13] Because no crystal structures of oligomers of the series Boc-(L-Phe-L-Oxd)_n-OBn were available, herein we show results for the crystallization of a mixture of two diastereoisomers with the general formula Boc-(Phe-Oxd)₂-OBn: Boc-(L-Phe-L-Oxd)₂-OBn (**1**) and Boc-L-Phe-L-Oxd-D-Phe-L-Oxd-OBn (**2**), in which the second Phe moiety has been replaced with its enantiomer, D-Phe.

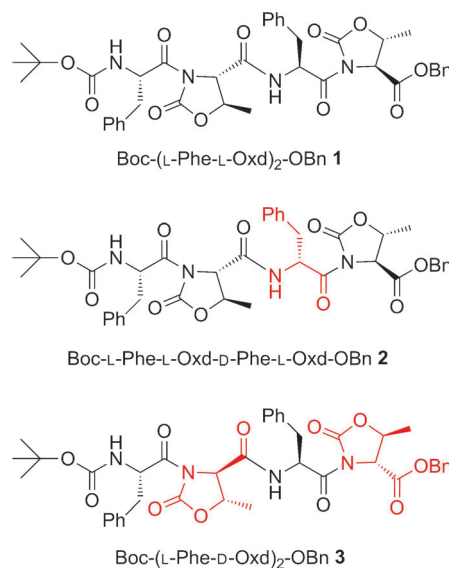
We obtained interesting information on the preferential conformations of **1** and **2** and on the morphology of the **1**+**2** mixture in the solid state, as a function of the crystallization solvent, compared with the properties of the two pure epimers.

Part of the information on the preferred conformation of **1** and **2** in solution has been obtained through VCD analysis. These compounds have been compared with the known compound Boc-(L-Phe-D-Oxd)₂-OBn (**3**),^[3,14] the VCD spectrum of which had never been recorded.

Results and Discussion

Synthesis and sample preparation

We prepared the three oligomers **1**, **2**, and **3** (Scheme 1) by conventional methods in solution, starting from L-Phe, D-Phe, L-Thr, and D-Thr.



Scheme 1. Structure of the compounds described herein. The moieties of the D series are highlighted in red.

The isomers of general formula Boc-Phe-Oxd-OBn are prepared in high yield by the addition of Boc-L-Phe-OH or Boc-D-Phe-OH to L-Oxd-OBn^[15] or D-Oxd-OBn in the presence of *N*-[(¹*H*-benzotriazolyl)(dimethylamino)methylene]-*N*-methylmethaniminium hexafluorophosphate *N*-oxide (HBTU) and triethylamine (TEA) in dry acetonitrile,^[16] whereas both L-Oxd-OBn and D-Oxd-OBn moieties can be easily synthesized on a multigram scale starting from L-Thr.

The epimers **1**, **2**, and **3** were synthesized in solution. For the preparation of **1**, Boc-(L-Phe-L-Oxd)-OH was obtained by selective deprotection of the C-terminal benzyl ester of Boc-(L-Phe-L-Oxd)-OBn with H₂ in methanol in the presence of Pd/C (5%), and H-L-Phe-L-Oxd-OBn-CF₃CO₂H was prepared by cleavage of the N-terminal Boc moiety with anhydrous trifluoroacetic acid (TFA) in dichloromethane. The two deprotected moieties were then coupled by using HBTU and TEA in dry acetonitrile under an inert atmosphere to provide **1** in satisfactory yield. Following the same procedure with different Boc-Phe-Oxd-OBn moieties, compounds **2** and **3** were readily obtained. All of the deprotection steps were performed with excellent yields, although the yields for the coupling steps were between 85 and 90%.

Because the aim of the work was the preparation of crystals suitable for single-crystal X-ray diffraction, we tried to crystallize **1** by using several solvents and mixtures (methanol, isopropanol, diethyl ether, tetrahydrofuran, ethyl acetate, acetonitrile, ethyl *tert*-butyl ether, and various solvent mixtures), but we did not succeed. The crystallization of **2** under the same conditions also failed.

Thus, we prepared a 1:1 molar ratio mixture of **1** and **2** and tried to crystallize this mixture in the same solvents: the most promising results were obtained in methanol and isopropanol (two alcohols), and in diethyl ether and methyl *tert*-butyl ether (MTBE; two ethers). These solvents have different polarities (two are polar and two are less polar) and different sizes (two

Compound (20 mg, 17 mmol)	Solvent (2 mL)			
	MeOH	<i>i</i> PrOH	Et ₂ O	MTBE
1	A	B	C	D
2	E	F	G	H
1+2 (1:1 ratio)	I	J	K	L

are large and two are small). The samples were prepared in 12.5 mL sample vials, all of which contained a solution of **1**, **2**, or **1+2** (20 mg, 17 mmol) in a suitable solvent (2 mL), as summarized in Table 1.

Analysis by X-ray crystallography

After one week, all samples were completely dried and first analyzed by X-ray powder diffraction to check the presence of crystalline material. The powder diffraction patterns are reported in Figure 1 and show that only deposits of the mixture of

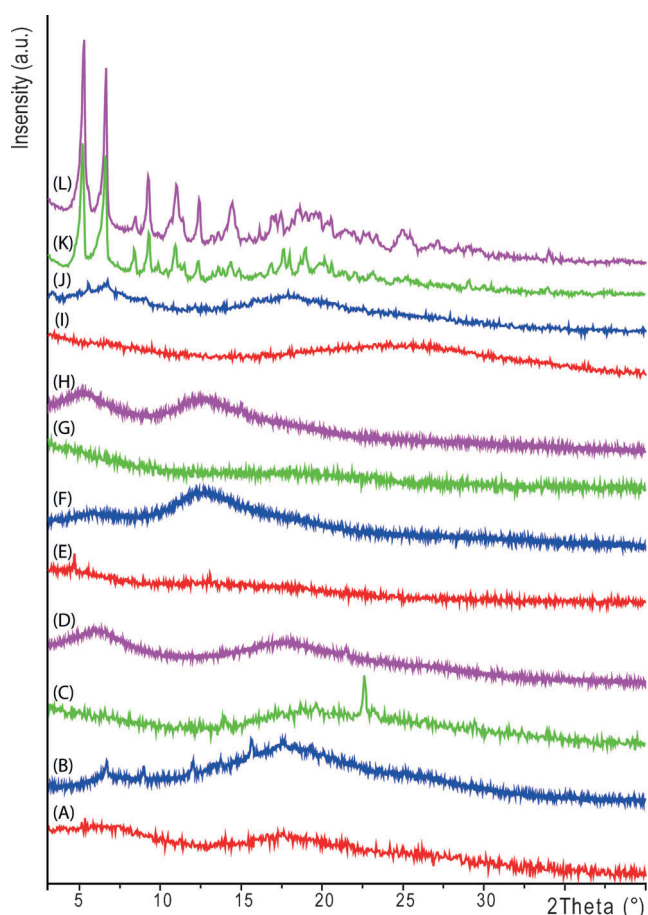


Figure 1. X-ray powder diffraction patterns of **1** (samples A, B, C, and D), **2** (samples E, F, G, and H) and a mixture of **1+2** (samples I, J, K, and L). The different solvents used in the precipitation experiments are indicated by different colors: methanol in red, isopropanol in blue, diethyl ether in green, and MTBE in purple.

1+2 precipitated from diethyl ether (sample K) or MTBE (sample L) are able to give clear and strong diffraction peaks.

These diffraction patterns present two strong peaks that correspond to periodicities of 16.9 and 13.4 Å, which appear also very weakly in the diffraction pattern of the mixture of **1+2** precipitated from isopropanol. These two long periodicities could be associated to the molecular packing of molecules **1** and **2**.

After these encouraging results, very slow crystallization of the mixture of **1+2** from MTBE afforded crystals suitable for single-crystal X-ray diffraction.^[17] The crystal structures of epimers **1** and **2** are shown in Figure 2a and b, respectively. Interestingly, one molecule of MTBE is present in the asymmetric unit in addition to **1** and **2**.

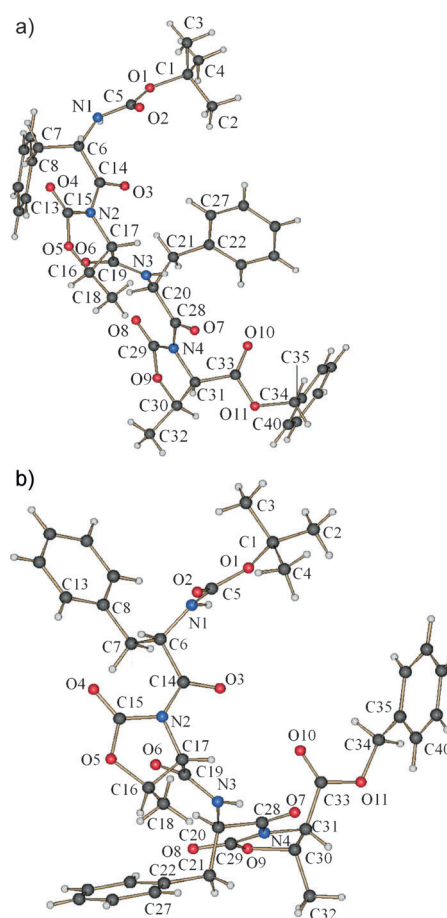
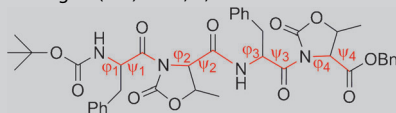


Figure 2. Crystal structures of **1** (a) and **2** (b).

The X-ray molecular structures of **1** and **2** exhibit some similarities, but inversion of the configuration at carbon C20 (*S* in **1** and *R* in **2**) has a significant impact on the backbone conformations. The ϕ and ψ torsion angles of all of the residues of **1** and **2** are given in Table 2 and compared with the same torsion angles of the reported crystal structure of **3**.

From inspection of the torsion angles, compound **1** shows the tendency to form a preferential distorted PPII conformation because the average torsion angles for a PPII helix are $\phi =$

Table 2. Selected backbone torsion angles (in °) for **1**, **2**, and **3**.



Compd	Phe		Oxd		Phe		Oxd	
	ϕ_1	ψ_1	ϕ_2	ψ_2	ϕ_3	ψ_3	ϕ_4	ψ_4
1	-72.8(3)	169.3(3)	-55.6(3)	138.8(2)	-138.0(3)	154.3(2)	-77.6(3)	176.7(2)
2	-79.3(3)	158.6(2)	-63.3(3)	151.1(2)	131.5(3)	-160.0(2)	-67.4(3)	173.9(2)
3	-134(2)	153(2)	51(2)	-148(2)	-133(2)	160(2)	57(2)	33(2)

-79° and $\psi = 150^\circ$. Indeed all of the ψ values range from 138.8 to 176.7°, whereas the ϕ values range from -55.6 to -77.6° , with the exception of ϕ_3 , which is -138.0° . The backbone torsion angles for L-Phe are $\phi_3 = -138.0^\circ$ and $\psi_3 = 154.3^\circ$ and correspond approximately to those in peptide β strands. A similar outcome was obtained for compound **2**, for which the backbone torsion angles of residue 3 had opposite signs because this residue was a D-Phe group; thus the preferred conformation of these short oligomers was very similar and differed only for ϕ_3 and ψ_3 , which had opposite signs. The preferred conformation of **1** is between a PPII helix and β strands; this suggests that a PPII helix will form for longer and more structured oligomers.

In contrast, compound **3**^[14] forms infinite antiparallel β -sheet structures, 15 of which are very different from the conformations **1** and **2**; thus showing the strong effect of the reversal of the absolute configuration of the Oxd moieties on the secondary structure of these hybrid foldamers.

The crystal-packing motif of the solvate cocrystal of **1**+**2** shows the formation of columns that run along the *a* axis in a parallel way, in which the two epimers, held together by classical N–H...O intermolecular hydrogen bonds, alternate as depicted in Figure 3. In particular, the N–H...O hydrogen bonds are exclusively between molecules **1** and **2** and the oxygen atoms involved in the two epimers are not equivalent. Mole-

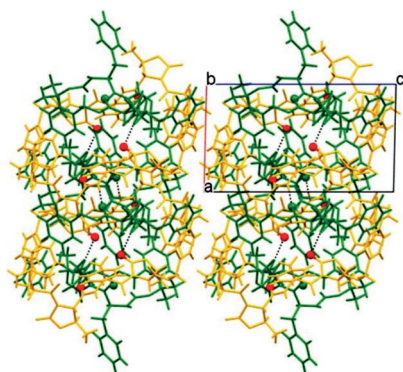


Figure 3. Perspective view of the crystal packing of the epimeric pair of **1** and **2** showing two of the columns that run along the *a* axis (the solvent molecules are not represented for the sake of clarity). Epimer **1** is dark yellow and epimer **2** is green. The oxygen atoms of **1** and **2** involved in the N–H...O hydrogen bonds (black dots) are drawn as spheres, which are red for **1** and green for **2**.

cule **1** is engaged in three N–H...O hydrogen bonds through the oxygen atoms O6 and O8 and the hydrogen atom bound to N3, whereas **2** establishes hydrogen bonds through O10 and the hydrogen atoms bound to N3 and N1 (see Table 3).

Solution conformational analysis

To check whether the preferred conformations found in the solid state were retained in solution, we analyzed compounds **1**, **2**, and **3** by the VCD tech-

Table 3. Intermolecular hydrogen bonding for the epimeric mixture **1**+**2**.^[a]

D–H...A	D–A	H...A	Angle D–H...A
N3A–H3N...O10B ^[b]	3.048(3)	2.19(2)	170(3)
N1B–H11N...O6A ^[b]	2.921(3)	2.08(2)	161(3)
N3B–H31N...O8A	3.121(3)	2.25(2)	175(3)

[a] D = hydrogen-bond donor, A = hydrogen-bond acceptor. [b] Symmetry codes: (') $x-1, y, z$; (") $x+1, y, z$. Epimers **1** and **2** have the same numbering scheme and are distinguishable by the final letters A (for **1**) and B (for **2**).

nique, using solvents not easily involved in hydrogen bonding (acetonitrile and chloroform). Indeed different behavior in crystallization may reflect a correspondingly different behavior in the preferred conformation in solution. VCD and other chiroptical spectroscopy techniques can give valuable information in this respect: for the systems under study, the presence of aromatic groups perturbs the UV spectroscopic region, which is usually very sensitive to secondary structures, and makes the UV–CD region hard to use; for this reason, vibrational spectroscopy techniques are unique for the characterization of peptide conformations in our case.^[18] An example of the use of VCD to investigate the structure of foldamers in solution has been recently reported.^[19]

Figure 4 gives the absorption and VCD spectra obtained in the mid-IR region for the three oligomers. These data show that a change in chirality of the third amino acid (Phe) does not have a great influence on the VCD spectra; instead, a change in chirality of the two Oxd moieties appears to invert the spectrum between $\tilde{\nu} = 1150$ and 1500 cm^{-1} and alters considerably the typical amide I shape characteristic of the secondary structure.

In the case of peptides, VCD spectra can give valuable information, even by simply correlating the data with that reported in the literature;^[20] however, here we have the additional difficulty of dealing with the oxazolidinone group. In this instance, DFT calculations may help.

A detailed analysis of the behavior of these peptides in solution is beyond the scope of this study, although future devel-

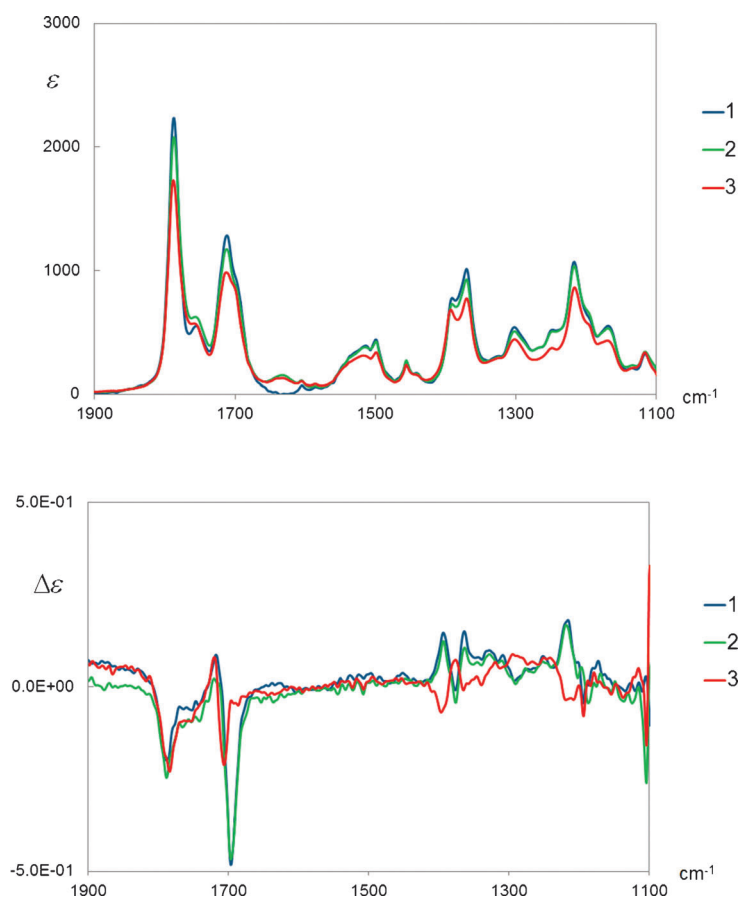


Figure 4. IR (top) and VCD (bottom) spectra of compounds **1**, **2**, and **3** in CD₃CN.

opments may be devoted to a thorough conformational study that takes into account calculated spectra of all possible conformers. Herein, we consider the structures obtained by optimizing those that result from the X-ray data. This will only give a rough indication, without aiming to give a strict correspondence between calculations and experiments, but we can consider DFT results as a guide to the discussion. Optimizations at the B3LYP/TZVP level give geometries similar to those in the crystal (see Supporting Information Figure S2); significant dihedral angles are reported in Table 4.

The spectra obtained with these geometries are reported in Figures S3–S5 in the Supporting Information. In Figure 5, we show a comparison of the three calculated VCD with the three

observed VCD spectra. From these calculations and from previous results,^[4] we note that, although for standard peptides the amide I band owing to the backbone carbonyl stretching is below $\tilde{\nu} = 1700 \text{ cm}^{-1}$, the presence of the alternating Oxd groups shifts the signal to higher wavenumbers ($\tilde{\nu} = 1713 \text{ cm}^{-1}$). The band recorded at $\tilde{\nu} = 1788 \text{ cm}^{-1}$ is due to the oxazolidinone carbonyl stretching and is not immediately related to the backbone conformation. From the calculations, we also see that vibrations of the aromatic moieties give contributions in the region of the amide II band (below $\tilde{\nu} = 1600 \text{ cm}^{-1}$).

Despite the use of only X-ray geometries (optimized) in DFT calculations, there is a nice correspondence between theory and experiments for the amide I band at $\tilde{\nu} = 1700 \text{ cm}^{-1}$ and for the features at wavenumbers lower than $\tilde{\nu} = 1300 \text{ cm}^{-1}$. This correspondence suggests a stiffness of these structures, owing to the bulky Phe groups and because oxazolidinone is much more rigid than proline.

Thus, as often performed for peptides,^[21] in the systems studied herein, the shape of the observed amide I bands also permit secondary-structure information to be obtained by simple correlations of recorded VCD data with what is already known in the literature.^[22] This has also been performed in the presence of D-peptides.^[23] Because the VCD sign pattern is dominated by the sense of the amide coupling in the helical conformation,^[24] we can argue that the couplet at $\tilde{\nu} = 1698\text{--}1725 \text{ cm}^{-1}$ (–, +) recorded for compounds **1** and **2** is indicative of a left-handed helix of PPII type. On the contrary, the low signal of compound **3** suggests a cancellation of PPII signals and is compatible with a beta structure (see Figure S2 in the Supporting Information).

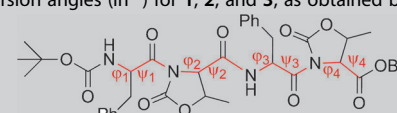
For completeness, we also recorded ECD spectra: again **1** and **2** exhibit almost identical CD spectra, and thus, similar behavior, whereas the alternating L-,D-peptide **3** has a clearly distinguishable spectrum (Figure 6).

Finally, we want to report the behavior of samples of **1**, **2**, and a mixture of **1** + **2** in the solid state crystallized from four solvents (methanol, isopropanol, diethyl ether, and MTBE).

Studies on the sample morphology

The morphology of the samples A–L (Table 1) was analyzed by SEM. All samples obtained from the crystallization of **1** or **2** in the four solvents afforded only the formation of solids that did not show any crystalline morphology or peculiar shape (see Figures S6 and S7 in the Supporting Information). In contrast, the mixture of **1** + **2**

Table 4. Selected backbone torsion angles (in °) for **1**, **2**, and **3**, as obtained by DFT optimization.



Compound	Phe		Oxd		Phe		Oxd	
	ϕ_1	ψ_1	ϕ_2	ψ_2	ϕ_3	ψ_3	ϕ_4	ψ_4
1	–75	161	–63	137	–124	155	–75	163
2	–77	153	–74	150	122	–156	–65	152
3	–109	144	56	–149	–134	159	63	26

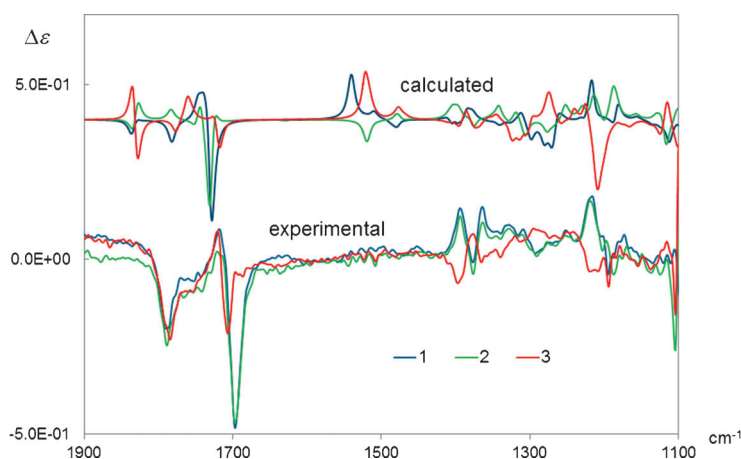


Figure 5. Comparison of calculated and experimental spectra of compounds **1**, **2**, and **3** (12 cm^{-1} bandwidth; wavenumber scaling factor 0.99).

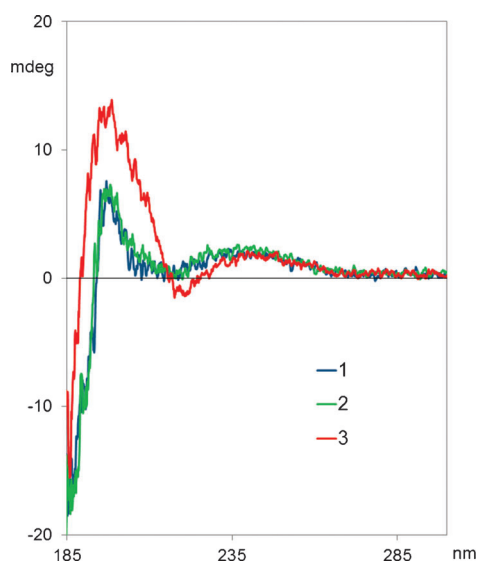


Figure 6. Superimposed CD spectra in the UV region for compounds **1**, **2**, and **3**.

showed a morphological selection that varied greatly from one solvent to another and was in agreement with the powder diffraction data. Images representative of the entire population of morphologies displayed by samples of **1** + **2** evaporated from methanol, isopropanol, diethyl ether, and MTBE are reported in Figure 7.

The precipitates from diethyl ether and MTBE are formed by aggregates of platelike crystals with variable thicknesses, ranging from 1 to $5\text{ }\mu\text{m}$, and areas. The precipitate from diethyl ether also shows the presence, as a minor phase, of needlelike particles (Figure 7K, inset). On the contrary, the mixture of **1** + **2** precipitated from isopropanol shows a fibrous structure, whereas that precipitated from methanol forms regular globular shapes that are unstable under the electron beam and generate a rough surface (Figure 7I, inset). This outcome suggests that these globes contain methanol, which quickly evaporates if the sample is heated; thus confirming the tendency of this

mixture to incorporate solvents, as already seen for the crystallization of the mixture in MTBE.

Conclusion

Through the crystallization of a 1:1 mixture of the two epimers **1** and **2** we have achieved several goals: 1) We found a useful method of obtaining crystals of a compound that would not crystallize in the pure form; this technique is currently being applied to the crystallization of longer oligomers. 2) The preferential conformation of both oligomers was fully elucidated and compared with the known conformation of **3**. 3) Conformational analysis of the three stereoisomers **1**, **2**, and **3** by VCD and ECD techniques in solution suggested that the preferred conformation found in the solid state was retained in solution. 4) Finally, we have demonstrated that the 1:1 mixture of **1** and **2** led to the formation of new materials with interesting and significantly different properties from the two pure compounds, such as the tendency to form crystals, fibers, and globules, depending on the solvent, and a general tendency to retain the solvent during the crystallization process.

Experimental Section

Synthesis: The melting points of the compounds were determined in open capillaries and are uncorrected. High-quality IR spectra (64 scans) were obtained at 2 cm^{-1} resolution by using a 1 mm NaCl solution cell and a Nicolet 380 FTIR spectrometer. All spectra were obtained as 3 mm solutions in dry CH_2Cl_2 at 297 K. All compounds were dried in vacuo and all sample preparations were performed in a nitrogen atmosphere. Routine NMR spectra were recorded with a Varian Inova 400 spectrometer at 400 (^1H) and 100 MHz (^{13}C). The measurements were performed in CD_3OD and in CDCl_3 . The proton signals were assigned by gCOSY spectra. Chemical shifts are reported in δ values relative to the solvent (CD_3OD or CDCl_3) signal.

Boc-(L-Phe-L-Oxd)₂-OBn (1): For synthetic details and characterization data, see ref. [4].

Boc-L-Phe-L-Oxd-D-Phe-L-Oxd-OBn (2): A mixture of H-L-Phe-L-Oxd-OBn-TFA (1 mmol)^[4] and Et_3N (3 mmol, 0.44 mL) in dry acetonitrile (10 mL) was added at room temperature to a stirred solution of Boc-L-Phe-D-Oxd-OH (1 mmol, 0.39 g)^[13] and HATU (1 mmol, 0.38 g) in dry acetonitrile (10 mL) under an inert atmosphere. The solution was stirred for 40 min under an inert atmosphere, then acetonitrile was removed under reduced pressure and replaced with ethyl acetate. The mixture was washed with brine, 1 N aqueous HCl ($3 \times 30\text{ mL}$), and 5% aqueous NaHCO_3 ($1 \times 30\text{ mL}$); dried over sodium sulfate; and concentrated in vacuo. The pure product was obtained after column chromatography on the silica gel (cyclohexane/ethyl acetate 8:2 as eluent) in 90% yield. M.p. = $83\text{--}84^\circ\text{C}$; $[\alpha]_D^{20} = -30$ ($c = 0.6$ in CHCl_3); $^1\text{H NMR}$ (400 MHz, CDCl_3): $\delta = 1.27\text{--}1.37$ (m, 15H; $2 \times \text{Me} + \text{tBu}$), 2.56–2.67 (m, 1H; CHH-Ph), 2.87–2.98 (m, 1H; CHH-Ph), 3.12–3.24 (m, 2H; $2 \times \text{CHH-Ph}$), 4.22 (d, $^3J(\text{H,H}) = 4.8\text{ Hz}$, 1H; CHN-Oxd), 4.28 (d, $^3J(\text{H,H}) = 3.3\text{ Hz}$, 1H; CHN-Oxd), 4.33–4.43 (m, 1H, CHO-Oxd), 4.43–4.51 (m, 1H, CHO-Oxd), 4.76 (brs, 1H, NH), 5.08 (s, 2H, OCH_2Ph), 5.48–5.61 (m, 1H, CHN- CH_2Ph), 5.72–5.83 (m, 1H, CHN- CH_2Ph), 7.01 (d, $^3J(\text{H,H}) = 9.2\text{ Hz}$, 1H;

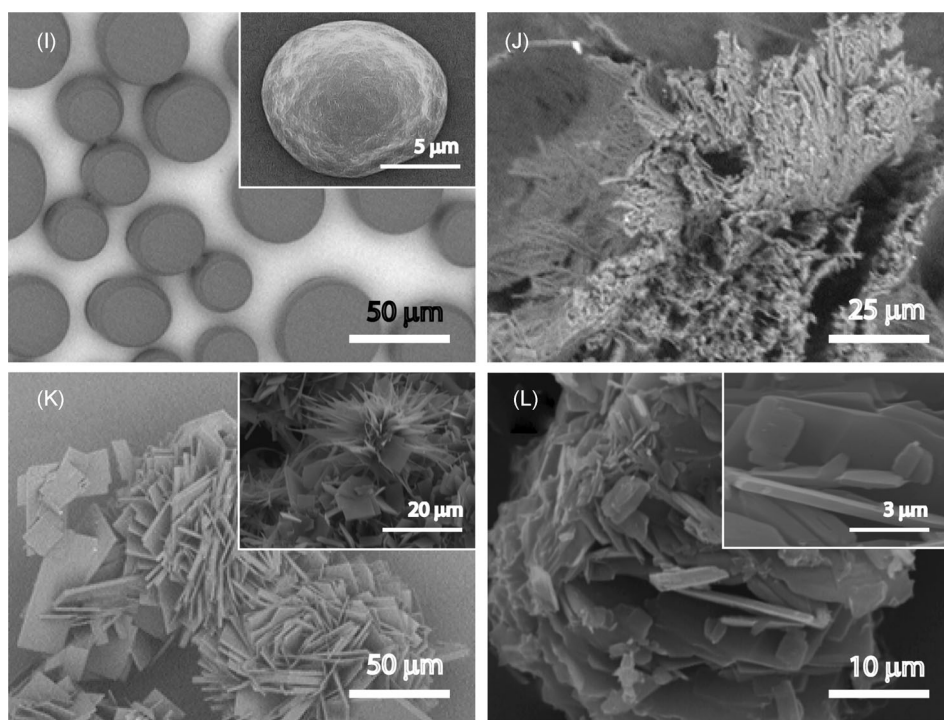


Figure 7. SEM pictures of the mixture of **1 + 2** precipitated from methanol (I), isopropanol (J), diethyl ether (K), or MTBE (L). The insets provide high-magnification images.

NH), 7.09–7.34 ppm (m, 15H, 3×Ph); ^{13}C NMR (CDCl_3): δ = 20.3, 20.9, 21.0, 28.2, 37.5, 37.7, 54.0, 61.8, 62.9, 85.8, 67.8, 74.0, 79.8, 126.8, 127.1, 128.3, 128.4, 128.6, 128.7, 128.8, 129.4, 129.5, 129.6, 134.5, 134.6, 135.4, 135.6, 151.6, 155.1, 166.7, 167.2, 171.2, 173.3 ppm; IR (CH_2Cl_2 , 3 mm): $\tilde{\nu}$ = 3440, 3407, 1785, 1748, 1708 cm^{-1} ; elemental analysis calcd (%) for $\text{C}_{40}\text{H}_{44}\text{N}_4\text{O}_{11}$: C 63.48, H 5.86, N 7.40; found: C 63.49, H 5.88, N 7.43.

Boc-(L-Phe-D-Oxd)₂-OBn (3): For synthetic details and characterization data, see ref. [14].

X-ray diffraction analyses: Powder X-ray diffraction patterns were collected by using a PanAnalytical X'Pert Pro equipped with an X'Celerator detector powder diffractometer using $\text{Cu}_{\text{K}\alpha}$ radiation ($\lambda = 1.5418 \text{ \AA}$) generated at 40 kV and 40 mA. The instrument was configured with a $1/4^\circ$ divergence and $1/4^\circ$ antiscattering slits. A standard quartz sample holder 1 mm deep, 20 mm high, and 15 mm wide was used. The diffraction patterns were collected within the 2θ range from 3 to 40° with a step size ($\Delta 2\theta$) of 0.02° and a counting time of 30 s.

Single-crystal X-ray diffraction: Intensity data for the cocrystal solvate containing the **1 + 2** pair of epimers obtained from MTBE were collected by using a SMART Apex II diffractometer equipped with a CCD area detector using a graphite-monochromated $\text{Mo}_{\text{K}\alpha}$ radiation source ($\lambda = 0.71073 \text{ \AA}$). Cell dimensions and the orientation matrix were initially determined from a least-squares refinement on reflections measured in 3 sets of 20 exposures, collected in 3 different ω regions, and eventually refined against all data. A full sphere of reciprocal space was scanned by 0.3° ω steps. The software SMART^[25] was used for collecting frames of data, indexing reflections, and determining lattice parameters. The collected frames were then processed for integration by using SAINT^[25] software and an empirical absorption correction was applied with SADABS.^[26] The diffractometer was equipped with a cryocooling

device used to set the temperature at 100 K. The structure was solved by using the SIR-2004 package^[25] and was subsequently refined on the F^2 values by the full-matrix least-squares program SHELXL-97.^[23] All non-hydrogen atoms were refined anisotropically. The methyl, methylene, and aromatic hydrogen atoms were placed in calculated positions, constrained to ride on their parent atoms, and refined isotropically with $U_{\text{iso}}(\text{H}) = 1.2$ or $1.5U_{\text{eq}}(\text{C})$. The N–H and methine hydrogen atoms were located in difference Fourier maps and were refined with constraints on their positions and U_{iso} values. The absolute structure configuration was not determined from X-ray data, but was known from the synthetic route. One solvent molecule (MTBE) was present in the asymmetric unit. Crystallographic data and refinement parameters are reported in Table S1 in the Supporting Information.

CCDC-970270 contains the supplementary crystallographic data for this paper. These data can be obtained free of charge from The Cambridge Crystallographic Data Centre via www.ccdc.cam.ac.uk/data_request/cif.

IR and VCD spectra: IR and VCD spectra were measured on a JASCO FVS 6000 spectrometer in deuterated acetonitrile at concentrations of 0.022 M for compound **1**, 0.020 M for **2**, and 0.025 M for **3** in a BaF_2 cell with a path length of 0.2 mm. The resolution was 4 cm^{-1} , 4000 accumulations were taken, and the solvent spectrum was subtracted.

IR and VCD spectra: IR and VCD spectra were measured on a JASCO FVS 6000 spectrometer in deuterated acetonitrile at concentrations of 0.022 M for compound **1**, 0.020 M for **2**, and 0.025 M for **3** in a BaF_2 cell with a path length of 0.2 mm. The resolution was 4 cm^{-1} , 4000 accumulations were taken, and the solvent spectrum was subtracted.

ECD spectra: The CD spectra were recorded on a JASCO spectropolarimeter, model J-815SE, as 1.1 mm solutions in CH_3CN in a 0.1 mm quartz cuvette.

Computational methods: DFT calculations have been performed at the B3LYP/TZVP level, with the Gaussian 09 package.^[27] Harmonic frequencies, dipole, and rotational strengths have been calculated by following the magnetic field perturbation method.^[28] Frequencies have been scaled by a 0.99 constant factor; Lorentzian band shapes with a half width of 12 cm^{-1} were assumed.

SEM imaging: The SEM observations were conducted by using a PhenomTM microscope (FEI) for uncoated samples and a Hitachi FEG 6400 microscope for samples coated with gold.

Acknowledgements

We would like to thank the Italian "Ministero dell'Istruzione, dell'Università e della Ricerca" (MIUR) for financial support, under the auspices of the program PRIN 2010NRREPL_009. We thank the Computing Center CINECA, Via Magnanelli 6/3, 40033 Casalecchio di Reno (Bologna), Italy, for access to their computational facilities.

Keywords: biomaterials • circular dichroism • crystal growth • conformational analysis • foldamers

- [1] a) S. H. Gellman, *Acc. Chem. Res.* **1998**, *31*, 173–180; b) V. Azzarito, K. Long, N. S. Murphy, A. J. Wilson, *Nat. Chem.* **2013**, *5*, 161–173; c) D. W. Zhang, X. Zhao, J. L. Hou, Z. T. Li, *Chem. Rev.* **2012**, *112*, 5271–5316; d) T. A. Martinek, F. Fulop, *Chem. Soc. Rev.* **2012**, *41*, 687–702; e) W. S. Horne, *Expert Opin. Drug Discovery* **2011**, *6*, 1247–1262; f) L. K. A. Pilsl, O. Reiser, *Amino Acids* **2011**, *41*, 709–718.
- [2] D. J. Hill, M. J. Mio, R. B. Prince, T. S. Hughes, J. S. Moore, *Chem. Rev.* **2001**, *101*, 3893–4011.
- [3] G. Guichard, I. Huc, *Chem. Commun.* **2011**, *47*, 5933–5941.
- [4] G. Longhi, S. Abbate, F. Lebon, N. Castellucci, P. Sabatino, C. Tomasini, *J. Org. Chem.* **2012**, *77*, 6033–6042.
- [5] C. Tomasini, G. Luppi, M. Monari, *J. Am. Chem. Soc.* **2006**, *128*, 2410–2420.
- [6] G. Angelici, G. Luppi, B. Kaptein, Q. B. Broxterman, H.-J. Hofmann, C. Tomasini, *Eur. J. Org. Chem.* **2007**, 2713–2721.
- [7] a) J. M. Berg, N. W. Goffeney, *Methods Enzymol.* **1997**, *276*, 619–627; b) B. W. Matthews, *Protein Sci.* **2009**, *18*, 1135–1138; c) D. E. Hague, J. R. Idle, S. C. Mitchell, R. L. Smith, *Xenobiotica* **2011**, *41*, 837–843; d) W. Cai, J. Marciniak, M. Andrzejewski, A. Katrusiak, *J. Phys. Chem. C* **2013**, *117*, 7279–7285; e) F. Faigl, E. Fogassy, M. Nógrádi, E. Pólovicsb, J. Schindler, *Tetr.: Asymmetry* **2008**, *19*, 519–536.
- [8] B. L. Pentelute, Z. P. Gates, V. Tereshko, J. L. Dashnau, J. M. Vanderkooi, A. A. Kosiakoff, S. B. H. Kent, *J. Am. Chem. Soc.* **2008**, *130*, 9695–9701.
- [9] S. W. Wukovitz, T. O. Yeates, *Nat. Struct. Biol.* **1995**, *2*, 1062–1067.
- [10] a) T. O. Yeates, S. B. H. Kent, *Annu. Rev. Biophys.* **2012**, *41*, 41–61; b) K. Mandal, S. B. H. Kent, *NATO SPS Series A: Chem. Biol.* **2013**, 11–22; c) J. R. Banigan, K. Mandal, M. R. Sawaya, V. Thammavongsa, A. P. A. Hendrickx, O. Schneewind, T. O. Yeates, S. B. H. Kent, *Protein Sci.* **2010**, *19*, 1840–1849.
- [11] a) M. Kudo, V. Maurizot, B. Kauffmann, A. Tanatani, I. Huc, *J. Am. Chem. Soc.* **2013**, *135*, 9628–9631; b) C. Dolain, H. Jiang, J.-M. Léger, P. Guionneau, I. Huc, *J. Am. Chem. Soc.* **2005**, *127*, 12943–12951.
- [12] I. Saha, B. Chatterjee, N. Shamala, P. Balaram, *Biopolymers* **2008**, *90*, 537–543.
- [13] a) R. G. Kostyanovsky, E. N. Nikolaev, O. N. Kharybin, G. K. Kadorkina, V. R. Kostyanovsky, *Mendeleev Commun.* **2003**, *13*, 97–99; b) S. Reemers, U. Englert, *Inorg. Chem. Commun.* **2002**, *5*, 829–831; c) E. Vedejs, R. W. Chapman, S. Lin, M. Müller, D. R. Powell, *J. Am. Chem. Soc.* **2000**, *122*, 3047–3052; d) U. Englert, R. Härter, C. Hu, I. Kalf, X. Zheng, *Z. Kristallogr.* **2000**, *215*, 627–631; e) R. Misra, W. Wong-Ng, P.-T. Cheng, S. McLean, S. C. Nyburg, *J. Chem. Soc. Chem. Commun.* **1980**, 659–660; f) I. L. Karle, J. Karle, *J. Am. Chem. Soc.* **1966**, *88*, 24–27.
- [14] G. Angelici, G. Falini, H.-J. Hofmann, D. Huster, M. Monari, C. Tomasini, *Chem. Eur. J.* **2009**, *15*, 8037–8048.
- [15] a) E. Falb, A. Nudelman, A. Hassner, *Synth. Commun.* **1993**, *23*, 2839–2844; b) G. Luppi, C. Soffrè, C. Tomasini, *Tetr.: Asymmetry* **2004**, *15*, 1645–1650.
- [16] G. Angelici, G. Falini, H.-J. Hofmann, D. Huster, M. Monari, C. Tomasini, *Angew. Chem.* **2008**, *120*, 8195–8198; *Angew. Chem. Int. Ed.* **2008**, *47*, 8075–8078; for the preparation of several compounds in this series, see: C. Tomasini, G. Angelici, N. Castellucci, *Eur. J. Org. Chem.* **2011**, 3648–3669.
- [17] Very slow crystallization from deuterated chloroform afforded single crystals suitable for crystallographic determination of the molecular structure. Interestingly, we noticed that these oligomers also showed a different diffraction pattern that corresponded to altered polymorphs if the precipitation conditions were changed (solvent and rate of precipitation).
- [18] T. A. Keiderling, *Curr. Opin. Chem. Biol.* **2002**, *6*, 682–688.
- [19] T. Buffeteau, L. Ducasse, L. Poniman, N. Delsuc, I. Huc, *Chem. Commun.* **2006**, 2714–2716.
- [20] T. A. Keiderling in *Circular Dichroism: Principles and Applications* (Eds.: N. Berova, K. Nakanishi, R. A. Woody), Wiley, New York, **2000**, pp. 621–666.
- [21] J. L. Kulp, J. C. Owirutsky, D. Y. Petrovykh, K. P. Fears, R. Lombardi, L. A. Nafie, T. D. Clark, *Biointerphases* **2011**, *6*, 1–7.
- [22] T. A. Keiderling, R. A. G. D. Silva, G. Yoder, R. K. Dukor, *Bioorg. Med. Chem.* **1999**, *7*, 133–141.
- [23] a) W. Mästle, R. K. Dukor, G. Yoder, T. A. Keiderling, *Biopolymers* **1995**, *36*, 623–631; b) R. K. Dukor, T. A. Keiderling, *Biopolymers* **1991**, *31*, 1747–1761.
- [24] G. Shanmugam, P. L. Polavarapu, E. Láng, Z. Majer, *J. Struct. Biol.* **2012**, *177*, 621–629.
- [25] M. C. Burla, M. Caliandro, M. Camalli, B. Carrozzini, G. L. Casciarano, L. De Caro, C. Giacovazzo, G. Polidori, R. Spagna, *J. Appl. Crystallogr.* **2005**, *38*, 381–388.
- [26] G. M. Sheldrick, SHELXL-97, University of Göttingen, Göttingen (Germany), **1997**.
- [27] Gaussian 09, Revision A.1, M. J. Frisch, G. W. Trucks, H. B. Schlegel, G. E. Scuseria, M. A. Robb, J. R. Cheeseman, G. Scalmani, V. Barone, B. Menonucci, G. A. Petersson, H. Nakatsuji, M. Caricato, X. Li, H. P. Hratchian, A. F. Izmaylov, J. Bloino, G. Zheng, J. L. Sonnenberg, M. Hada, M. Ehara, K. Toyota, R. Fukuda, J. Hasegawa, M. Ishida, T. Nakajima, Y. Honda, O. Kitao, H. Nakai, T. Vreven, J. A. Montgomery, Jr., J. E. Peralta, F. Ogliaro, M. Bearpark, J. J. Heyd, E. Brothers, K. N. Kudin, V. N. Staroverov, R. Kobayashi, J. Normand, K. Raghavachari, A. Rendell, J. C. Burant, S. S. Iyengar, J. Tomasi, M. Cossi, N. Rega, J. M. Millam, M. Klene, J. E. Knox, J. B. Cross, V. Bakken, C. Adamo, J. Jaramillo, R. Gomperts, R. E. Stratmann, O. Yazyev, A. J. Austin, R. Cammi, C. Pomelli, J. W. Ochterski, R. L. Martin, K. Morokuma, V. G. Zakrzewski, G. A. Voth, P. Salvador, J. J. Dannenberg, S. Dapprich, A. D. Daniels, Ö. Farkas, J. B. Foresman, J. V. Ortiz, J. Cioslowski, D. J. Fox, Gaussian, Inc., Wallingford CT, **2009**.
- [28] a) P. J. Stephens, *J. Phys. Chem.* **1985**, *89*, 748–751; b) A. D. Buckingham, P. W. Fowler, P. A. Galwas, *Chem. Phys.* **1987**, *112*, 1–14; c) J. R. Cheeseman, F. J. Devlin, M. J. Frisch, P. J. Stephens, *Chem. Phys. Lett.* **1996**, *252*, 211–220.

Received: September 2, 2013

Published online on November 8, 2013